

### **Articles**

https://doi.org/10.20884/1.jm.2025.20.3.11655

# Structural Insights into Mutant and Wild-Type InhA Proteins: Implications for Targeting Tuberculosis and the Role of NAD Cofactors

Ryscha Dwi Iryani, Faozan Ahmad, Zahra Silmi Muscifa, Setyanto Tri Wahyudi\*

Department of Physics, Faculty of Mathematics and Natural Sciences, IPB University, Bogor 16680, Indonesia.

\*Corresponding author email: stwahyudi@apps.ipb.ac.id

Received March 22, 2023; Accepted July 22, 2025; Available online November 20, 2025

ABSTRACT. The high death rate and prevalence of multidrug-resistant tuberculosis (MDR-TB) pose a significant global health challenge. Enoyl-acyl carrier protein reductase (InhA) from *Mycobacterium tuberculosis* is one of the main targets for drug development to treat tuberculosis. Wever, mutations in the InhA structure found in *Mycobacterium tuberculosis* are responsible for MDR-TB. The Protein Data Bank (PDB) 3D structure of InhA was used in this study. The PDB has 102 3D structures, with 77 structures for wild-type proteins and 25 structures for mutant proteins. The structures with the best resolution values and most favorable region statistics in Ramachandran plots were selected, and redocking and cross-docking simulations were performed with Autodock Vina software to study the binding affinity of protein-ligand complexes and to assess the impact of mutations on binding affinity. This research also provides insights into the influence of Nicotinamide Adenine Dinucleotide (NAD) cofactors, which increase ligand binding efficiency. The results show how important the NAD cofactor is for improving ligand binding and how mutations can change the therapeutic potential of the found ligands. They also give suggestions for structures that can be used to make drugs that fight multidrug-resistant tuberculosis. Based on the docking results, with an RMSD value of less than 2.00 Å, the structures recommended for the virtual screening stage are 5COQ, 5CP8, and 5OIF for mutant proteins and 2X23, 4BQP, 4D0S, 4OHU, 4OXK, 4TRJ, and 5MTR for the wild-type protein.

Keywords: Autodock Vina, Enoyl-acyl carrier protein reductase (InhA), multidrug-resistant tuberculosis (MDR-TB), NAD, Tubercolosis.

#### INTRODUCTION

Tuberculosis (TB) continues to be a substantial worldwide health concern, with approximately 5.8 million instances of pulmonary TB documented in 2020 (Villar-Hernández et al., 2023). Tuberculosis (TB) is a prominent cause of sickness and mortality globally, despite extensive attempts to control its transmission. This poses a serious public health burden, especially in countries like Indonesia, where it is a major concern (Noviyani et al., 2021). Transmission of the disease occurs by airborne particles expelled by individuals with tuberculosis during coughing or sneezing. Therefore, it is imperative to devise efficient public health policies and healthcare interventions to address this persistent menace (World Health Organization, 2023).

Enoyl Acyl Carrier Protein Reductase (InhA) is a crucial enzyme in the life cycle of *Mycobacterium tuberculosis*, the pathogenic bacterium responsible for tuberculosis. This enzyme is vital in the synthesis of mycolic acids, which are important constituents of the bacterial cell wall. These acids enhance the strength and pathogenicity of the bacterium (Prasad

et al., 2021). The mechanism of action of the antituberculosis medicine isoniazid, which specifically targets InhA by binding to it and disrupting the synthesis of mycolic acid, has been extensively investigated. This interaction highlights significance of InhA as a focal point for the development efficacious therapeutics of for tuberculosis, providing a means to combat the tuberculosis-causing bacterium (Marrakchi et al., 2000).

The rise of multidrug-resistant tuberculosis (MDR-TB) presents a major obstacle to global health, highlighting immediate requirement the innovative therapeutic approaches (Chowdhury et al., 2023). The resistance emerges when Mycobacterium tuberculosis develops resistance to traditional anti-TB treatment drugs, making outcomes complicated. One of the potential targets for the creation of novel drugs is InhA, a protein that plays a significant role in pathways that lead to drug resistance. This study employs computational methods to uncover novel information about the composition of TBC InhA, hence facilitating the creation of medications to combat existing drug

resistance. The purpose is to offer information regarding the receptor that can be utilized for computer-aided drug discovery. This work employed the ensemble docking approach to reevaluate the interactions between proteins and ligands inside complex structures obtained from the Protein Data Bank (PDB) with a focus on TB. This procedure entails the selection of pertinent protein-ligand complexes and the execution of redocking simulations to recreate and assess the original binding positions. InhA plays a crucial role in the life cycle of Mycobacterium TB, the pathogenic bacterium responsible for tuberculosis. This enzyme is important for the synthesis of mycolic acids, which are critical constituents of the bacteria's cell wall. Mycolic acids are responsible for enhancing the strength and pathogenicity of the bacterium (Prasad et al., 2021). The mechanism of action of the anti-tuberculosis medicine isoniazid, which specifically targets InhA by binding to it and disrupting the synthesis of mycolic has been extensively researched. interaction highlights the significance of InhA as a focal point for the development of potent TB therapies, providing a means to combat the TBcausing microorganism (Marrakchi et al., 2000).

### EXPERIMENTAL SECTION Material

In this study, computational analyses were performed using a Personal Computer with the following specifications: a 64-bit Windows 10 Home Single Language operating system. The software suite utilized included PyMOL for molecular visualization, Autodock Tools and Autodock Vina for molecular docking simulations (Rauf et al., 2015), SwissModel for homology modeling (Waterhouse et al., 2018), and Microsoft Excel for data analysis. The protein data set comprised 11 wild-type protein structures and 7 mutant variants, which were selected based on their relevance to the research objectives.

#### Method

#### Selection for 3D structure

The InhA protein sequence was obtained from using the access code P9WGR1 (https://www.uniprot.org/uniprotkb/P9WGR1/entry) on October 15, 2023, and served as the primary for identifying relevant 3D structures. Based on this entry, a total of 102 structures which consist 77 wild-type and 25 mutant were retrieved **RCSB** Protein Data (https://www.rcsb.org) using the keyword "InhA." The PDB ID, ligand identity, and X-ray resolution of each structure were directly obtained from the RCSB database. The type classification (wild-type or mutant) verified using sequence and annotations from UniProt.

From this dataset, 18 representative structures (11 wild-type and 7 mutant) were selected for further analysis. Filtering was based on structural

completeness, biological relevance to Mycobacterium tuberculosis, and resolution quality ( $\leq 2.50$  Å). To ensure stereochemical accuracy, Ramachandran plot statistics and G-Factor values were assessed using PROCHECK software (Laskowski et al., 1993). Only structures with >90% of residues in the most favored regions and G-Factor values >0 were retained. These quality indicators, along with resolution, ligand data, and type classification, are summarized in **Table 1**.

#### **Protein Preparation**

#### Structural improvement using swissmodel

Most of the InhA protein structures are singlechain monomers, although some are tetramers, as shown in Figure 1A, Only Chain A was selected for this analysis due to its complete residue sequence and optimal binding site representation. Figure 1B illustrates the suitability of Chain A for molecular docking studies, as it contains the active site region where both NAD and inhibitor molecules typically bind. The binding site highlighted in Figure 1D corresponds to previously reported interaction sites involved in the inhibition of mycolic acid biosynthesis which essential process for Mycobacterium tuberculosis (Prasad et al., 2021).

Protein structure preparation was conducted using PyMOL, where all water molecules were removed, hydrogen atoms were added, and the protein was separated from its co-crystallized ligands to avoid interference in docking. For structures with incomplete residues (e.g., PDB codes 4BII, 4DOS, 3FNE, and 4UVH), missing amino acids were modeled and refined using SwissModel to ensure completeness and reliable binding site representation.

### Alignment structure to the selected reference structure.

The selection of protein structures for this study underwent meticulous organization and screening to guarantee their high quality. Utilizing statistical analysis of the Ramachandran plot, protein conformations were assessed to ensure adherence to physical and geometric principles. **Table 1** highlights the selection of protein structure PDB code 2X23 as the reference, chosen for its superior Ramachandran plot statistics and high-resolution quality.

Figure 2 illustrates the structural alignment of InhA proteins using PyMOL, with PDB ID 2X23 as the reference structure. Point Α displays superimposition of wild-type InhA structures, while point B shows the alignment of mutant variants. The high degree of overlap among the backbone conformations in both panels reflects structural conservation across the datasets, validating the suitability of 2X23 as a reference. Structural alignment helps ensure that docking analyses are conducted on comparable binding site orientations, thereby minimizing structural bias. This step is essential in comparative docking studies, especially when evaluating ligand binding across different conformations or mutations. It provides confidence that observed differences in docking scores or binding poses are due to molecular interactions rather than large-scale structural inconsistencies (Kufareva & Abagyan, 2011).

After alignment, a root mean square deviation (RMSD) value (**Table 2**) shows how much the wild-

type and mutant protein structures deviate from the reference structure. A smaller RMSD value indicates high similarity of the protein structure to the reference structure. We compared wild-type and mutant protein structures to the reference. The protein structure with PDB code 4TRJ closely matches the reference, with an RMSD value below 2.00 Å in all 18 structures examined.

Table 1. Best InhA structure determined by Resolution and Ramachandran Plot Analysis

PDB ID	Type Proteins	Resolution (Å)	Most favored regions (%)	G-Factor	Ligand ID
2X23	Wild-Type	1.81	92.1	0.11	TCU_1
4BII	Wild-Type	1.95	92.5	0.15	PYW_1
4TRJ	Wild-Type	1.73	91.6	0.16	665
4OHU	Wild-Type	1.60	91.7	0.23	2TK
4OXK	Wild-Type	1.84	92.0	0.25	1\$5
4UVH	Wild-Type	1.89	92.4	0.16	UUD
40IM	Wild-Type	1.85	90.2	0.24	JUS
4D0S	Wild-Type	1.64	91.9	0.17	9G4
3FNE	Wild-Type	1.98	90.3	0.01	8PC
5MTR	Wild-Type	2.00	91.6	0.02	XTO
4BQP	Wild-Type	1.89	91.6	0.14	VMY
2NV6	Mutant	1.90	92.0	0.09	ZID
5OIF	Mutant	2.03	92.4	0.12	9W5
5COQ	Mutant	2.30	91.5	0.17	TCU 2
5CP8	Mutant	2.40	90.2	0.15	TCU <sup>-</sup> 3
50IM	Mutant	1.91	91.1	0.18	9VZ
4BGE	Mutant	2.25	91.5	0.12	PYW_2
4BGI	Mutant	2.09	91.6	0.10	141

Note: TCU\_1, TCU\_2, TCU\_3, and PYW\_1 and PYW\_2 show structures with different PDB codes but have co-crystal ligands with the same code. To differentiate the co-crystal ligands, we give additional numbers.

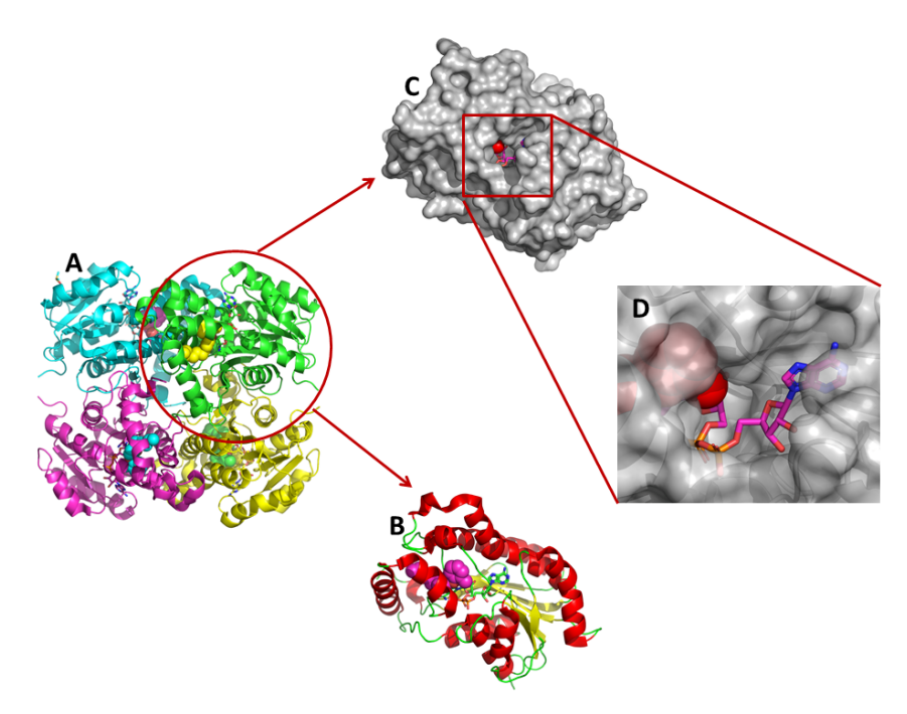


**Figure 1.** PDB Code 2X23 Structure: **A)** Chains A, B, E, and G are green, cyan, magenta, and yellow. **B)** Chain A 3D. **C)** Chain A binding site molecular surface. **D)** Magnified binding site.

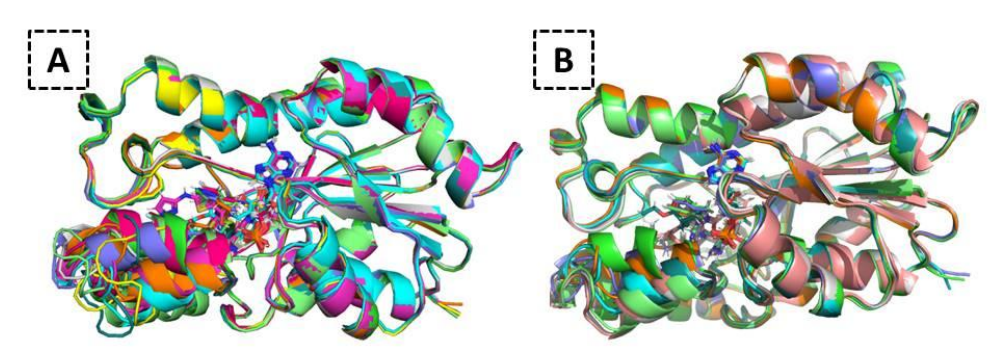


**Figure 2.** Protein structure alignment against reference (2X23) using PyMOL; (A) wild-type protein alignment; and (B) mutant protein alignment.

**Table 2.** Proteins structural alignment versus reference structure (2X23). Sorted by smallest RMSD.

PDB	RMSD	Protein	
2X23	0	Wild-Type	
4TRJ	0.174	Wild-Type	
4OHU	0.186	Wild-Type	
4OXK	0.194	Wild-Type	
4UVH	0.203	Wild-Type	
40IM	0.208	Wild-Type	
4D0S	0.212	Wild-Type	
3FNE	0.217	Wild-Type	
5MTR	0.223	Wild-Type	
2NV6	0.238	Mutant	
5OIF	0.245	Mutant	
4BQP	0.263	Wild-Type	
5COQ	0.268	Mutant	
5CP8	0.270	Mutant	
50IM	0.325	Mutant	
4BII	0.347	Wild-Type	
4BGE	0.415	Mutant	
4BGI	0.547	Mutant	

# Re-Docking process of wild-type and mutant protein structures

The docking procedure has two crucial steps to understand how Nicotinamide Adenine Dinucleotide (NAD) affects the InhA protein, which is important in tuberculosis. Initially, NAD is added to the InhA protein structure and is subsequently removed. This rigorous methodology compares affinity energy measurements to reveal NAD's cofactor role. Comparisons help explain enzyme function and medication interactions at the molecular level.

Many biological functions, including metabolism and energy production, require NAD, a cofactor. As a cofactor ligand in the InhA protein structure, it is essential to TB metabolic activities. Note that PDB IDs 4BGE, 4BGI, and 2NV6 are structures that lack NAD. Adding NAD to the InhA structure is essential for studying its biological interactions. In PDB code 2NV6, NAD's unique conformation with the ligand creates ZID, highlighting protein structural interactions. These relationships help explain the protein's function and how medications target it.

#### Protein preparation and docking simulation

PyMol was used to prepare proteins by adding hydrogen atoms for hydrogen bonding and water removal. After Gasteiger's partial charge assignment, proteins were prepared for AutoDock simulations. Hydrogen atoms are commonly lacking in crystal formations; therefore, docking calculations must include them. AutoDock tools translated the cocrystallized ligand and receptor into \*.pdbqt format and set docking parameters using a 20x20x20 grid box for re-docking.

Then, AutoDock Vina calculated ligand-receptor binding affinity to assess interaction strength. An increasingly negative value denotes high binding affinity, whereas a value close to zero or increasingly positive denotes low binding affinity. Lower RMSD results indicate less conformational changes in docked ligands compared to co-crystal ligands. Additionally, ligand affinity was measured to determine receptor binding efficiency. Cross-docking is part of the docking ensemble and derives from other ligands (Camila et al., 2014). Cross-docking is

carried out by docking each co-crystal ligand to all protein structures used, both wild-type and mutant structures; this method can also be called ensemble docking. The docking results of each ligand against the entire structure are then averaged. Cross-docking was used to find the optimum co-crystal ligand for wild-type and mutant protein structures to acquire the best affinity value for 3D protein structures.

#### **Ligand Efficiency Calculation**

Ligand Efficiency (LE) measures how effectively a ligand utilizes the number of heavy atoms in generating binding energy for its target. The definition of a heavy atom calculated in LE is a nonhydrogen atom (Hopkins et al. 2014). LE is determined experimentally using Equation 1, where R represents the universal gas constant of 1.987  $\times$ 10<sup>-3</sup> kcal·mol<sup>-1</sup>·K<sup>-1</sup>, T denotes the temperature in Kelvin, and Kd signifies the dissociation constant (in molarity, M). N<sub>HA</sub> denotes the Number of Heavy Atoms. Since  $\Delta G$  can be calculated by  $RTlnK_d$ , therefore in the molecular docking calculation, LE can be calculated using Equation 2 where  $\Delta G$  is the binding energy in kcal mol<sup>-1</sup>.

$$LE = \left(-2.303 \left(\frac{RT}{N_{HA}}\right)\right) \times log K_d \tag{1}$$

$$LE = \frac{-\Delta G}{N_{HA}} \tag{2}$$

$$LE = \frac{-\Delta G}{N_{HA}} \tag{2}$$

The high ligand efficiency indicates the potential for greater binding affinity enhancement of the drug design (Perola, 2010).

#### A Comparative Analysis of Re-Docking and Cross-**Docking Outcomes**

Cross-docking and re-docking are used to find the protein structure with the highest energy affinity during docking. Comparing ligands' docking results with wild-type and mutant protein structures helps choose the best structure and stable co-crystal ligand for docking. Mutations may alter the binding affinity between the ligand and the receptor owing to missing residues in the protein structure. Table 3 lists mutant protein mutation locations.

### **RESULTS AND DISCUSSION**

#### **Determination Center coordinates**

The docking center was determined based on the location of co-crystallized present in the selected PDB structures. These ligands are known to bind near the active site of InhA, particularly around essential residues. For structures that lacked co-crystallized ligands, the active site was inferred through structural alignment with homologous ligand-bound structures to ensure consistency and biological relevance.

center coordinates used in docking simulations were defined using AutoDockTools grid box settings, which require precise center x, y, and z coordinates for each protein. These coordinates are provided in Table 4. Following structural alignment, all docking and cross-docking simulations were initiated from these defined points, thereby focusing the simulation on the biologically relevant binding pocket. To ensure methodological consistency, the same docking center coordinates were applied for structures with or without NAD to maintain consistency across comparative analyses and ensure precision in ligand binding predictions.

#### ReDocking Assessment: The Role of NAD

Redocking investigations show that negative ligand-receptor affinity values increase binding interactions. The affinity and RMSD values in Figures 3 and Figures 4 show redocking with and without NAD. The protein with the highest affinity for NAD was 5MTR, -11.61 kcal/mol, whereas 4BII had the lowest affinity, -2.92 kcal/mol. 5MTR affinity was reduced to -9.93 kcal/mol without NAD, while 4BII affinity dropped but not significantly to -2.68 kcal/mol. In general, the redocking of wild-type protein structures yields elevated binding affinity values in the presence of NAD, while a reduction in binding affinity is seen in the absence of NAD. Only one structure, 4UVH, had distinct yet inconsequential outcomes. It is evident from this observation that NAD plays an important role in the process of InhA protein-ligand binding.

This observation is consistent with the biological role of NAD as a universal enzyme cofactor that plays a crucial role in redox reactions and is essential for the catalytic activity of many oxidoreductases. In various proteins, NAD binding is often associated with increased ligand affinity, enhancing both enzymatic function and inhibitor effectiveness (Cahn et al., 2017; Rawat et al., 2003). In Mycobacterium tuberculosis, NAD forms a covalent binding with isoniazid (INH) resulting in the INH-NAD complex, which binds tightly to the InhA enzyme and disrupts mycolic acid synthesis. This interaction significantly improves inhibitory efficiency. Mutations near the NAD binding site, such as \$94A, can reduce the efficiency of INH-NAD complex formation or lower binding affinity, contributing to decreased therapeutic effectiveness (Vilchèze & Jacobs, 2007).

Furthermore, RMSD measurements reveal cocrystalline ligand structural alignment before and after redocking. Generally, values below 2.00 Å indicate little structural changes. The RMSD values for PDB codes 4BII, 3FNE, and 4UVH surpassed the threshold, with values of 5.461 Å, 9.115 Å, and 5.375 Å, respectively. This high RMSD value is thought to be caused by structural variations caused by the insertion of amino acid residues during the structure improvement process using SWISS-MODEL.

Figure 4 shows affinity energy differences for redocking mutants with and without NAD cofactor unlike Figure 3. The ligands, redocking structure with the NAD ligand shows that PDB code 2NV6 has -9.67 kcal/mol affinity. This indicates that PDB code 2NV6 has the highest affinity energy.

**Table 3**. Mutation position in Mutant Structures.

PDB Code	Location of Mutation
50IM	T2A
5OIF	T2A
4BGI	S94A
5COQ	V203A
5CP8	I215A
4BGE	S94A
2NV6	S94A

**Table 4.** Center coordinates for redocking of wild-type and mutant protein structures.

PDB	Types of Proteins	Χ	Υ	Z
2X23	Wild-type	-20.633	-4.357	-30.290
4BII	Wild-type	-18.065	-5.831	-34.370
4BQP	Wild-type	-18.268	-2.053	-31.820
4D0S	Wild-type	-21.550	-4.254	-30.900
4OHU	Wild-type	-20.586	-4.435	-30.320
40IM	Wild-type	-20.730	-3.760	-29.890
4OXK	Wild-type	-20.259	-3.654	-30.570
4TRJ	Wild-type	-19.872	-4.468	-31.240
3FNE	Wild-type	-20.789	-4.217	-30.570
4UVH	Wild-type	-17.420	1.128	-30.445
5MTR	Wild-type	-20.570	-4.901	-31.210
2NV6	Mutant	-22.353	1.028	-27.015
4BGE	Mutant	-22.183	-3.634	-29.540
4BGI	Mutant	-22.340	-3.621	-29.590
5COQ	Mutant	-20.675	-4.244	-30.280
5CP8	Mutant	-20.546	-4.431	-30.500
5OIF	Mutant	-20.155	-1.436	-29.980
50IM	Mutant	-19.136	-1.401	-30.030
Average		-19.764 ± 1.400	-3.442 ± 1.942	-30.601 ± 1.389

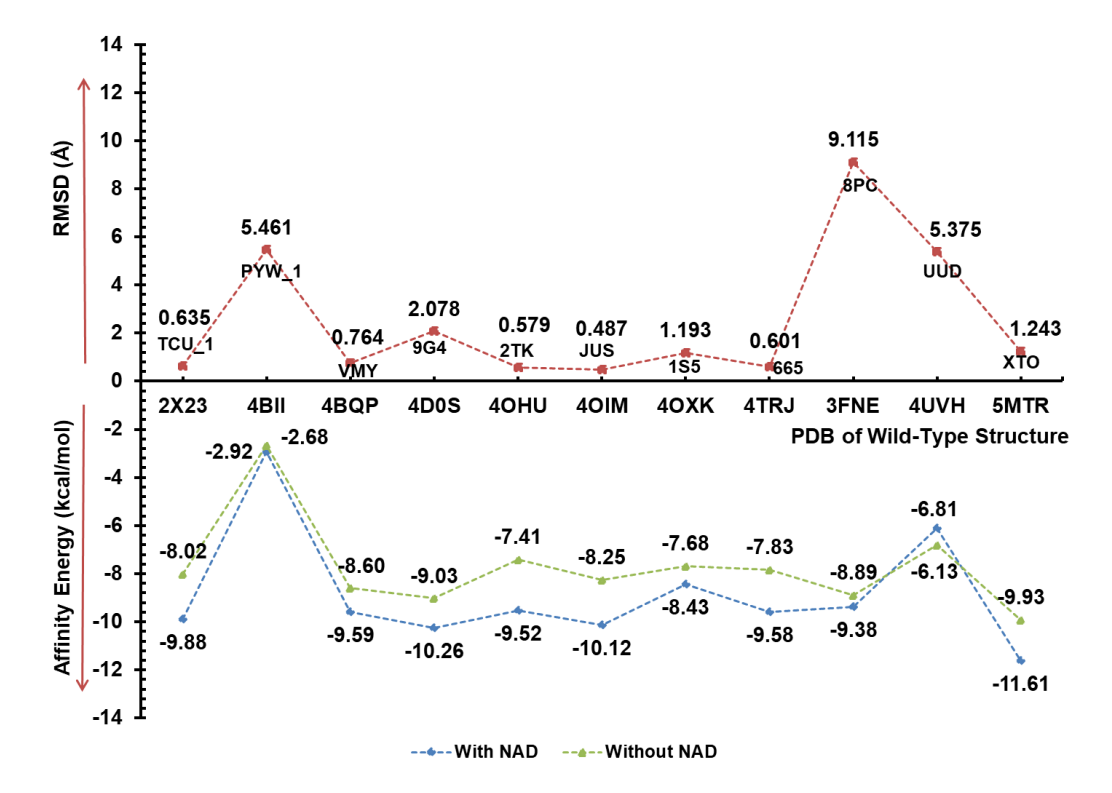


Figure 3. Graph of affinity energy values and RMSD resulting from redocking of wild-type protein

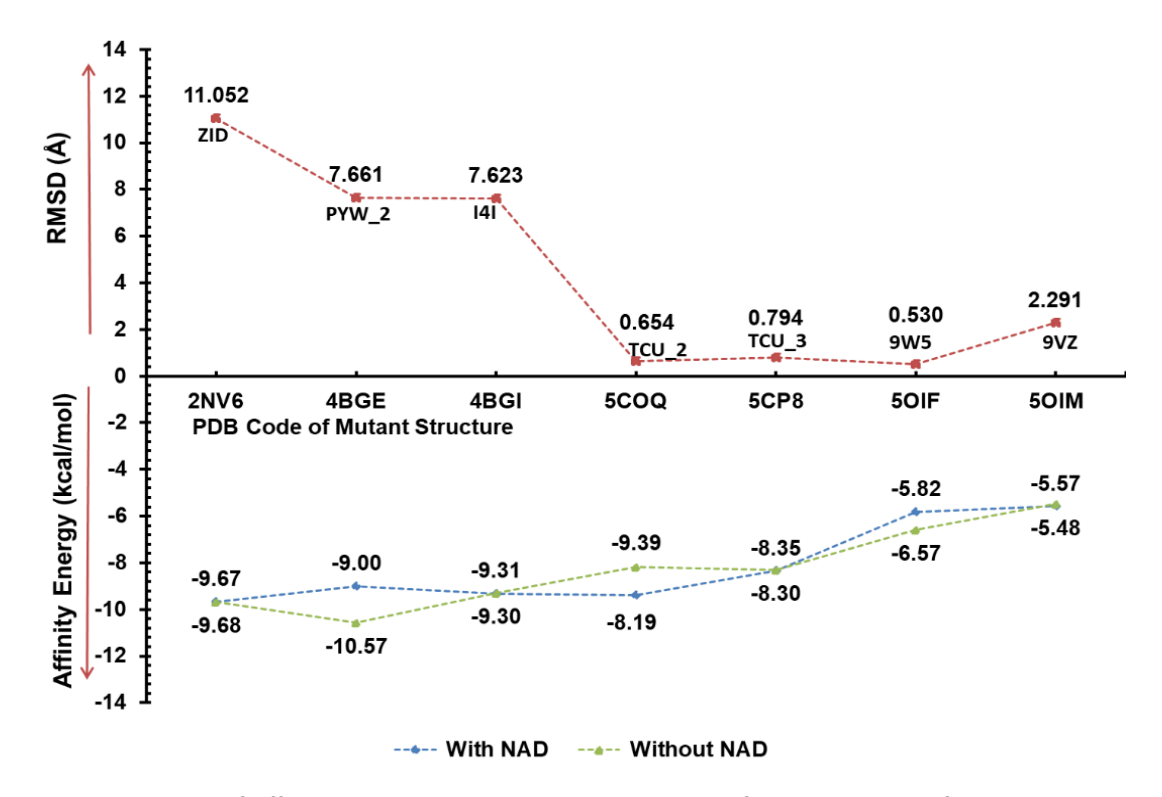


Figure 4. Graph of affinity energy values and RMSD resulting from redocking of mutant protein.

The affinity of the redocking result without the NAD ligand is only 0.01 kcal/mol lower than the result, which is -9.68. No substantial modification has occurred due to structure redocking.

PDB code 4BGE has the lowest affinity energy of 10.57 kcal/mol in redocking without NAD ligands. Redocking with NAD ligand yields an affinity energy of -9.00 kcal/mol in PDB code 4BGE. These structures vary greatly. The Protein Data Bank (RSCB) crystal structures of 4BGE and 2NV6 lack NAD ligands. NAD ligands add little affinity energy to both structures. Adding NAD ligand helps bind ligand and InhA protein.

Mutant protein structure (RMSD) values vary. Of the 7 redocked structures, 3 (PDB codes 5COQ, 5CP8, and 5OIF) demonstrated values < 2.00 Å. PDB codes 2NV6, 4BGE, 4BGI, and 5OIM yield values of 11.052 Å, 7.661 Å, 7.623 Å, and 2.291 Å.

# Cross-docking Assesment: Affinity average and ligand efficiency

Cross-docking has been widely applied to evaluate binding site adaptability and ligand specificity across different receptor conformation (Thomas et al., 2022). In this study, cross-docking was used to assess the reproducibility and robustness of ligand-binding predictions across multiple InhA protein structures. This method is commonly employed in molecular docking studies to determine ligand compatibility with various receptor conformations. Its effectiveness in drug discovery workflows has also been demonstrated in evaluating binding consistency and supporting pharmacophore modeling (Ganesan & Karthikeyan, 2021).

Cross-docking utilizes the x, y, and z coordinates of a center to determine the average outcomes of Redocking. Cross docking employs NAD ligands. We determined the affinity by performing cross-docking of the co-crystallized ligand with both the wild-type and mutant protein structures. The affinity energy value is being compared to the efficiency of the ligand as measured by pIC50.

The 4D0S ligand efficiency with the 9G4 ligand has the highest value of 0.730 kcal/mol/atom and an affinity energy of -10.26 kcal/mol. The lowest efficiency ligand for the wild-type protein was the 4OIM structure with the JUS ligand. The ligand efficiency value obtained by 4OIM is 0.331 kcal/mol/atom while the affinity energy is -10.12 kcal/mol.

This is different from the ligand efficiency value in the wild-type protein structure. In the mutant structure, the PDB 4BGE coded protein with the PYW ligand produces the highest ligand efficiency value, 0.447 kcal/mol/atom, with an affinity value of -9.00 kcal/mol. Meanwhile, the lowest efficiency ligand value is in the protein structure coded PDB 2NV6 with a ZID ligand of 0.186 kcal/mol/atom with an affinity value of -9.67 kcal/mol.

### Cross-docking Assesment: Comparison Results on Wild-Type and Mutant Structure

This approach uses docking simulations to find stable co-crystalline ligands. The ligand is stable when binding to wild-type and mutant protein structures with the lowest average affinity energy.

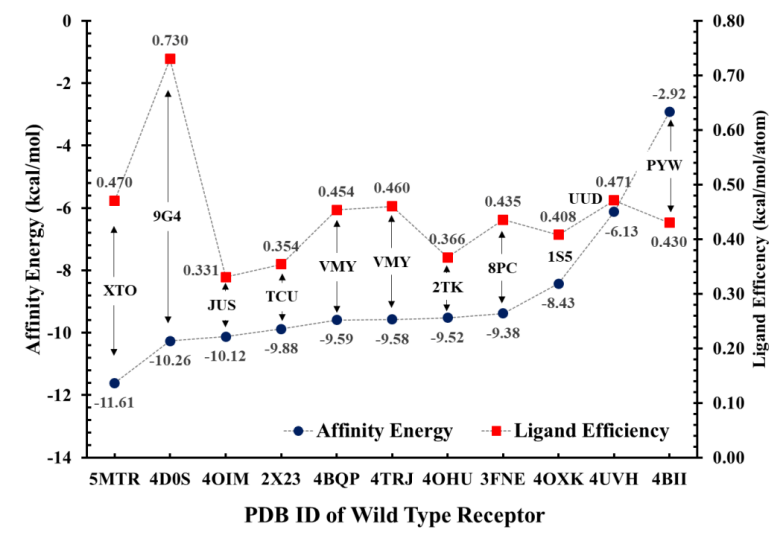


Figure 5. Average affinity and ligand efficiency of wild-type receptor structure

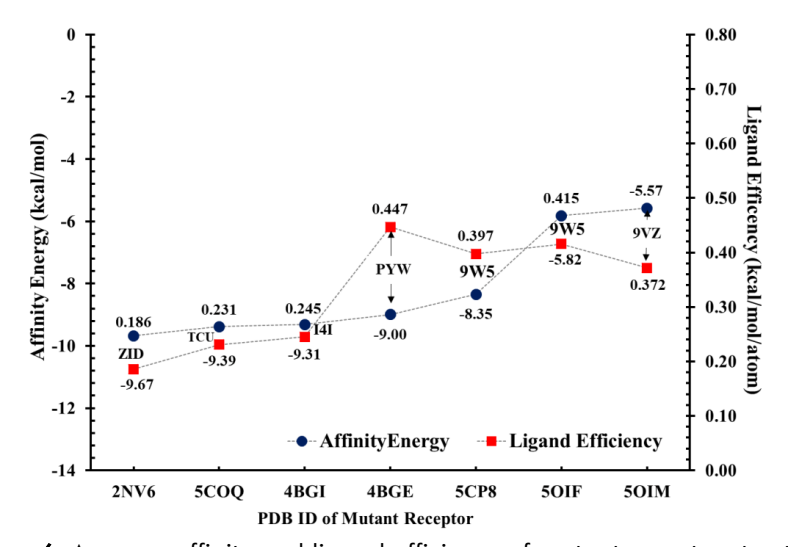
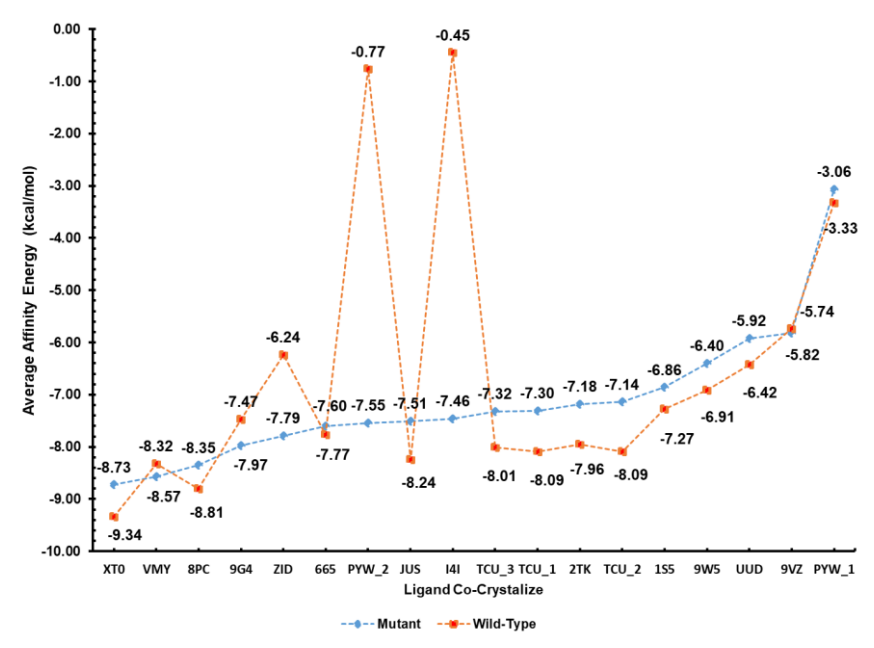


Figure 6. Average affinity and ligand efficiency of mutant receptor structure



**Figure 7.** Graph of the average affinity energy values resulting from cross-docking on wild-type proteins TCU\_1, TCU\_2, and TCU\_3 are co-crystallized ligands of 2X23, 5COQ, and 5CP8, respectively. While PYW\_1 and PYW\_2 are co-crystallized ligands of 4BII and 4BGE.

The comparison of the results in **Figure 7** is made based on mutant protein data followed by wild-type data. The goal is to find the best and the worst ligand that can interact with both the mutant and wild-type structures. Among ligands, the XTO ligand has the highest affinity for the wild-type structure, -9.34 kcal/mol. It also has the highest affinity for the mutant structure, -8.73 kcal/mol. The XTO ligand binds well to wild-type and mutant proteins. XTO is a protein co-crystallization ligand with PDB code 5MTR. The binding affinity of the PYW\_1 ligand is the lowest among all ligands, both in its interaction with the wild-type structure (-3.33 kcal/mol) and in its interaction with the mutant structure (-3.06 kcal/mol). The co-crystall ligand PYW\_1 is present in the 4BII structure.

Typically, the binding affinity of ligands is greater when they engage with the structures of the wild-type protein, while a decrease in affinity is observed when ligands interact with the structures of the mutant protein. The wild-type and mutant exhibit modest variations in affinity values for three ligand structures, namely VMY, 9G4, and ZID. Nevertheless, it is worth noting that there exist two ligands, namely PYW\_2 and I4I, that exhibit exceptional affinity values when engaging with both wild-type and mutant proteins.

TCU ligands (TCU\_1, TCU\_2, and TCU\_3) that were originally coupled to three protein structures (2X23, 5COQ, and 5CP8) had steady values of -8.09, -8.09, and -8.01 kcal/mol when docked to the wild-type structure but declined with affinities of -7.30, -7.14, and -7.32 when interacted with mutants. Mutations in the InHA protein affect inhibitor binding. According to this data, the three TCUs docked in the wild-type structure vary slightly. The three also differed slightly when interacting with the mutant structure. This explains how the TCU ligand can maintain conformational stability in the interaction despite its distinct 3-dimensional structure from the PDB code.

Figure 7 shows PYW\_2 and I4I as outlier ligands. The average affinity of these two ligands for wild-type protein structures is close to zero, indicating poor interaction. Both structural protein mutants, 4BGE and 4BGI, co-crystallize with these two ligands. Hartkoorn et al. discovered these two structures and the wild-type 4BII structure with the PYW\_1 ligand. Visual examinations of 4BGE and 4BGI structures retrieved from the PDB Bank show that they lack NAD, unlike 4BII. In general, the InHA structure has a cofactor NAD. We think PYW\_2 and I4I have a low affinity for the wild-type structure because the native structure lacks NAD.

#### Effect of Mutation Position and ZID Structure

The identification results of the mutation results show a detailed analysis of amino acid residues that have undergone mutations (**Figure 7**). The impact of these mutations on the binding affinity between amino acids and co-crystalline ligands is significant.

Specifically, mutations outside the binding site generally led to a higher affinity value for the protein-ligand interaction than mutations close to the cocrystal ligand, as observed in PDB structures 2NV6, 4BGE, 4BGI, and 5COQ (Figure8). Conversely, the PDB structure 5CP8, with a mutation outside the binding site, exhibits a higher affinity value, indicating that the mutation's location is critical in influencing affinity energy (Figure 8).

Mutations often cause drug or ligand resistance in protein structures. For example, the S94A mutation found in the binding site of the InhA protein in PDB codes 2NV6, 4BGE, and 4BGI directly affects the interaction between the receptor and the ligand, thereby influencing the affinity energy value. Previous studies have demonstrated that the S94A mutation interferes with the formation or stability of the INHadduct, significantly decreasing isoniazid efficacy (Vilchèze et al., 2006; Rawat et al., 2003). These three PDB structures lack NAD ligands, resulting in comparatively better affinity values than other mutant structures. Among these, PDB 2NV6 with the ZID ligand exhibits the lowest affinity value, attributed to the mutation's precise location within the binding site and its proximity to the ZID ligand. This is consistent with previous findings suggesting that absence or disruption of NAD binding alters the structural integrity of the active site, consequently impacting ligand docking outcomes (Rawat et al., 2003)

The docking results of ZID ligands, PYW\_2, TCU\_2, TCU\_3, and I4I, with mutant and wild-type structures, further illustrate the impact of mutations on binding efficiency. For instance, the ZID ligand shows a higher affinity value when bound to the wild-type structure (-6.24 kcal/mol) than the mutant structure (-7.79 kcal/mol). Similarly, the PYW\_2 and I4I ligands demonstrate significant differences in affinity values between wild-type and mutant structures, highlighting how the S94A mutation affects the average affinity energy value and, consequently, the binding capability between the ligand and the protein structure.

We got the best redocking results with the PDB code 2NV6 and the mutant protein. This code had an affinity energy of -9.68 kcal/mol with its ZID cocrystalline ligand. However, cross-docking results vary significantly; the interaction of ZID with the wildtype protein yields an average affinity energy of -6.24 kcal/mol, while its interaction with the mutant protein results in a more favorable average of -7.79 kcal/mol. This suggests that the ZID ligand, an NIZ (isoniazid) and NAD complex, binds more effectively to its native site on the mutated InhA protein. NIZ code This is because the ZID structure is an adduct structure between Isoniazid and NAD (Figure 9). The ZID structure displays a fused molecule in which the nicotinamide ring of NAD is covalently bonded to the hydrazine group of isoniazid, forming the INH-NAD

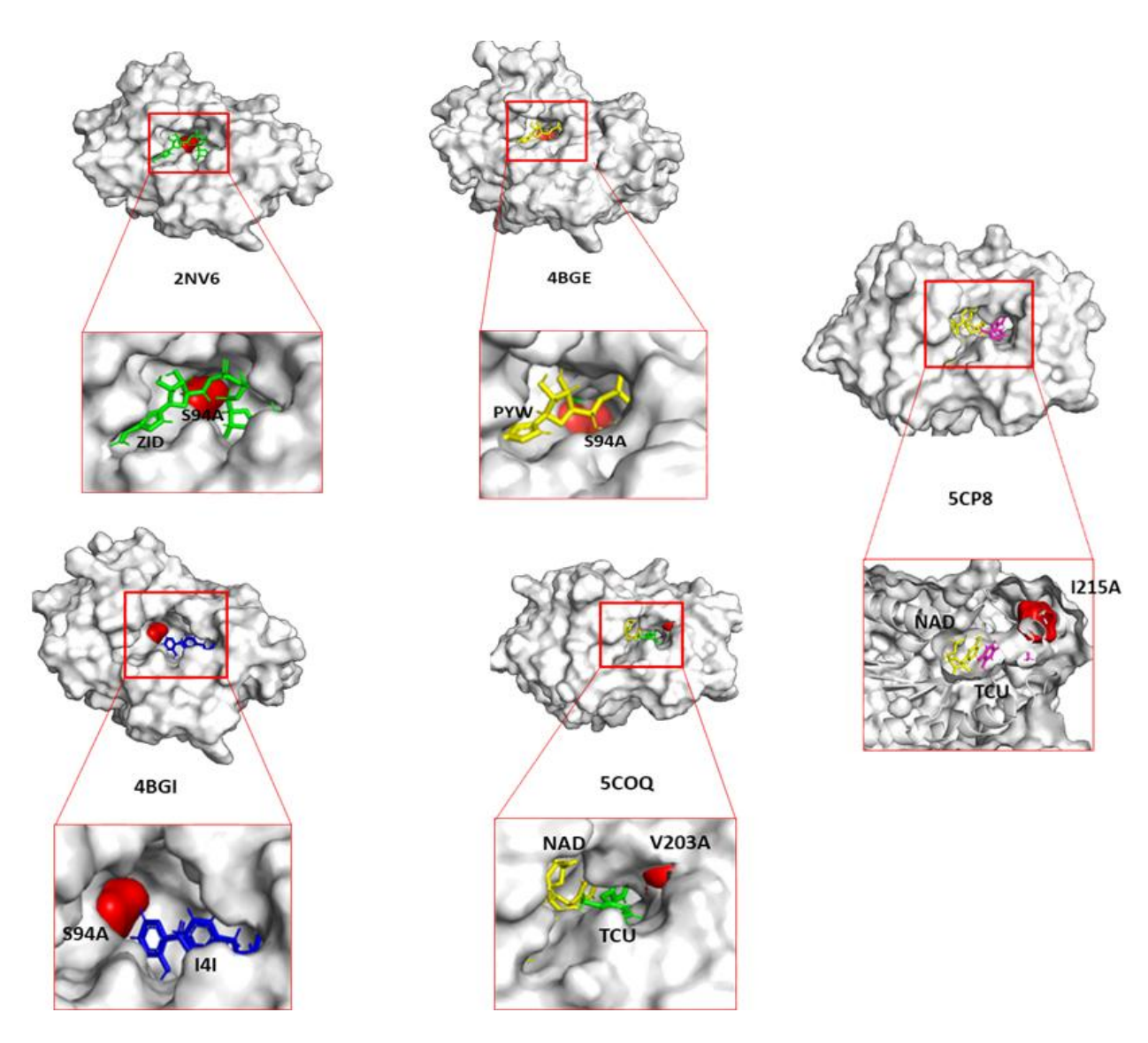
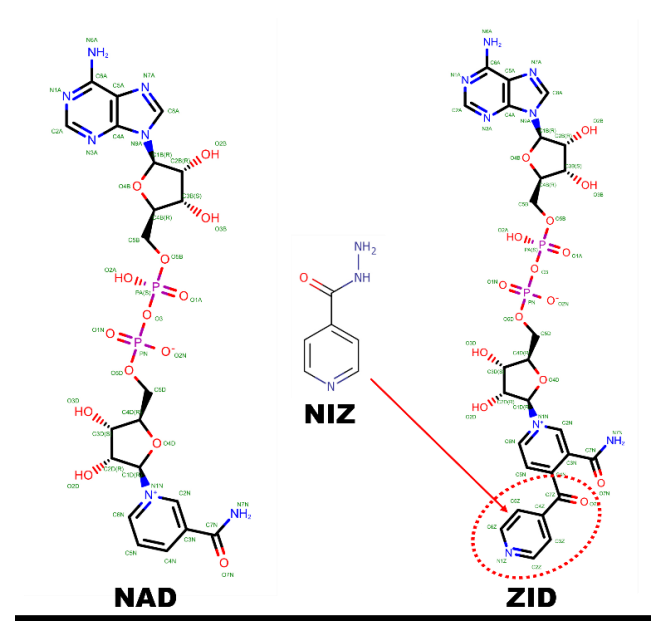


Figure 8. Location of mutation position in the mutant protein structure. Red is the location of the mutation.



**Figure 9.** Comparison between NAD, Isonizid (NIZ) with drugbank code: DB00951, ZID, Adduct between Isoniazid and NAD

adduct as a result of prodrug activation (Jena et al., 2015). In contrast, NIZ (isoniazid) and NAD exist as separate, non-adduct molecules. This distinction is relevant in docking simulations: while ZID represents the post-activation complex, using NIZ (DrugBank DB00951) and NAD separately offers more flexibility and biological accuracy in virtual screening, especially when modeling pre-binding or competitive inhibition scenarios (Dias et al., 2007). The NIZ code as Isoniazid is found in the PDB 6CFQ structure. We suggest that for docking simulations on InhA, not using the ZID-NAD Adduct structure, but using the NIZ structure with separate NAD.

#### **CONCLUSIONS**

The study's results provide novel perspectives on the structure of TBC inhA through the application of ensemble docking techniques, which in this paper were applied by cross-docking, which successfully created representative data. This work emphasizes the substantial impact of the NAD cofactor on the affinity of ligand binding and its crucial significance in the design of drugs. Moreover, this work elucidates the influence of mutations in the InhA enzyme on drug resistance, offering vital insights into the possible ramifications for medication effectiveness.

The presence of the NAD cofactor ligand in the re-docking outcomes resulted in a higher degree of affinity compared to the findings obtained without the NAD ligand. Incorporating the NAD ligand into a structure that originally lacks it will enhance the interaction between the ligand and the protein. The docking results indicate that the structures 5COQ, 5CP8, and 5OIF are suggested for the virtual screening step of mutant proteins, as they have a ligand RMSD value of less than 2.00 Å. The preferred architectures for wild-type proteins are 2X23, 4BQP, 4D0S, 4OHU, 4OXK, 4TRJ, and 5MTR.

Although the findings offer valuable insights, this study has limitations. The docking simulations used are based on static structures and do not consider protein flexibility or the effects of water and movement in real biological systems. In future studies, molecular dynamics simulations and lab experiments can help confirm these results and give a more complete understanding. It would also be useful to test other mutations that may affect drug resistance.

#### **REFERENCES**

Cahn, J. K. B., Werlang, C. A., Baumschlager, A., Brinkmann-Chen, S., Mayo, S. L., & Arnold, F. H. (2017). A general tool for engineering the NAD/NADP cofactor preference of oxidoreductases. *ACS Synthetic Biology*, 6(2), 326–333. https://doi.org/10.1021/acssynbio.6b00188

- Camila, S., Almeida, D.M., Helio, J., & Dardenne, L. E. (2014). A dynamic niching genetic algorithm strategy for docking highly flexible ligands. *Information Sciences*: 289. doi: 10.1016/j.ins.2014.08.002.
- Chowdhury, K., Ahmad, R., Sinha, S., Dutta, S., & Haque, M. (2023). Multidrug-Resistant TB (MDR-TB) and Extensively Drug-Resistant TB (XDR-TB) Among Children: Where We Stand Now. *Cureus*, 15(2). https://doi.org/10.7759/CUREUS.35154
- Dias, M. V. B., Vasconcelos, I. B., Prado, A. M. X., Fadel, V., Basso, L. A., de Azevedo Jr., W. F., & Santos, D. S. (2007). Crystallographic studies on the binding of isonicotinyl-NAD adduct to wild-type and isoniazid resistant 2trans-enoyl-ACP (CoA) reductase Mycobacterium tuberculosis. Journal Structural 159(3), 369-380. Biology, https://doi.org/10.1016/j.jsb.2007.04.009
- Ganesan, S., & Karthikeyan, C. (2021). Validation through re-docking, cross-docking and ligand enrichment in various well-resoluted MAO-B receptors. *International Journal of Pharmaceutical Sciences and Research*, 12(6), 3236–3244. https://doi.org/10.13040/ IJPSR.0975-8232.12(6).3236-44
- Hartkoorn, R. C, Pojer, F., Read, J.A., Gingell, H., Neres, J., Horlacher, O.P., Altmann, K.H., Cole,S.T. (2014). Pyridomycin bridges the NADH- and substrate-binding pockets of the enoyl reductase InhA. *Nat Chem Biol. 10*: 96-98, doi: https://doi.org/10.1038/nchembio.1405
- Hopkins, A. L., Keseru, G. M., Leeson, P. D., Rees, D. C., & Reynolds, C. H. (2014). The role of ligand efficiency metrics in drug discovery. Nat. Rev. Drug Discov. 13. 105.
- Jena, L., Deshmukh, S., Waghmare, P., Kumar, S., & Harinath, B. C. (2015). Study of mechanism of interaction of truncated isoniazid-nicotinamide adenine dinucleotide adduct against multiple enzymes of *Mycobacterium tuberculosis* by a computational approach. *International journal of mycobacteriology*, 4(4), 276–283. https://doi.org/10.1016/j.ijmyco.2015.06.006
- Laskowski, R. A., MacArthur, M. W., Moss, D. S., & Thornton, J. M. (1993). PROCHECK: A program to check the stereochemical quality of protein structures. *Journal of Applied Crystallography*, 26(2), 283–291. https://doi.org/10.1107/S0021889892009944
- Lovell, S. C., Davis, I. D., Arendall, W. B., de Bakker, P. I., Word, J. M., Prisant, M. G., & Richardson, D. J. (2003). Structure validation by cα geometry: φ, ψ and cβ deviation. Proteins: *Structure, function, and bioinformatics, 50*(3), 437-450. https://doi.org/10.1002/prot.10286.

- Kufareva, I., & Abagyan, R. (2012). Methods of protein structure comparison. *Methods in molecular biology* (Clifton, N.J.), 857, 231– 257. https://doi.org/10.1007/978-1-61779-588-6 10
- Marrakchi, H., Lanéelle, G., & Quémard, A. (2000). InhA, a target of the antituberculous drug isoniazid, is involved in a mycobacterial fatty acid elongation system, FAS-II. *Microbiology (Reading, England)*, 146 (Pt 2)(2), 289–296. https://doi.org/10.1099/00221287-146-2-289.
- Noviyani, A., Nopsopon, T., & Pongpirul, K. (2021). Variation of tuberculosis prevalence across diagnostic approaches and geographical areas of Indonesia. *PLoS ONE*, *16*(10). https://doi.org/10.1371/JOURNAL.PONE.025 8809
- Perola, E. (2010). An analysis of the binding efficiencies of drugs and their leads in successful drug discovery programs. J. Med. Chem. 53. 2986–2997.
- Prasad, M. S., Bhole, R. P., Khedekar, P. B., & Chikhale, R. V. (2021). Mycobacterium enoyl acyl carrier protein reductase (InhA): A key target for antitubercular drug discovery. *Bioorganic Chemistry*, 115.
- Rauf, M. A., Zubair, S., & Azhar, A. (2015). Ligand docking and binding site analysis with pymol and autodock/vina. *IJBAS*. 4(2). 168-177. doi: 10.14419/ijbas.v4i2.4123.
- Thomas, B. N., Parrill, A. L., & Baker, D. L. (2022). Self-docking and cross-docking simulations of

- G protein-coupled receptor-ligand complexes: Impact of ligand type and receptor activation state. *Journal of Molecular Graphics and Modelling*, 112, 108119. https://doi.org/10.1016/j.jmgm.2021.108119
- Rawat, R., Whitty, A., & Tonge, P. J. (2003). The isoniazid-NAD adduct is a slow, tight-binding inhibitor of InhA, the *Mycobacterium tuberculosis* enoyl reductase: Adduct affinity and drug resistance. *Proceedings of the National Academy of Sciences of the United States of America, 100*(24), 13881–13886.
- Vilchèze, C., & Jacobs, W. R., Jr. (2007). The mechanism of isoniazid killing: Clarity through the scope of genetics. *Annual Review of Microbiology*, 61, 35–50.
- Villar-Hernández, R., Ghodousi, A., Konstantynovska, O., Duarte, R., Lange, C., & Raviglione, M. (2023). Tuberculosis: current challenges and beyond. *Breathe*, 19(1). https://doi.org/10.1183/20734735.0166-2022
- Waterhouse, A., Bertoni, M., Bienert, S., Studer, G., Tauriello, G., Gumienny, R., T. Heer, F., de Beer, T. A. P., Rempfer, C., Bordoli, L., Lepore, R., & Schwede, T. (2018). SWISS-MODEL: homology modelling of protein structures and complexes. *Nucleic Acids Research.* 46. doi: 10.1093/nar/gky427.
- World Health Organization. (2023). *Global Tuberkulosis Report 2023*. World Health Organization.